Semicond. Sci. Technol. **28** (2013) 105003 (8pp) doi:10.1088/0268-1242/28/10/105003

Modified Airy function method modelling of tunnelling current for Schottky barrier diodes on silicon carbide

A Latreche[1,3] **and Z Ouennoughi**[2]

[1] Département de sciences de la Matière, Université de Bordj Bou Arreridj, Algerie
[2] Laboratoire optoélectronique et composants, Département de physique, UFAS Sétif, Algérie

E-mail: hlat26@yahoo.fr

Received 11 May 2013, in final form 11 May 2013
Published 25 July 2013
Online at stacks.iop.org/SST/28/105003

Abstract
We present a simple method for analysing the tunnelling current through Schottky barrier diodes on SiC, based on the modified Airy function (MAF) approach. The MAF method is accurate for linear-shaped barriers which is the case for the top of the Schottky barrier diodes. The results have been compared with those obtained by the conventional Wentzel–Kramers–Brillouin (WKB). This study proves that the WKB method is valid for the Schottky barrier diodes with and without the incorporation of Schottky barrier lowering under low or high bias voltage.

1. Introduction

Silicon carbide is currently of great interest in high-voltage power devices. Its properties of high critical field strength, reasonable carrier mobilities, wide band gap, and high thermal conductivity make it a useful material for high-frequency, high-temperature, and high-power devices [1, 2]. However, due to the high electric fields normally encountered in SiC devices, the reverse leakage current of Schottky diodes can be significantly enhanced prior to junction breakdown due to the tunnelling mechanism [3]. The high electric fields encountered in SiC and other wide band gap materials lead to significant tunnelling through the Schottky barrier, thus increasing the leakage current by many orders of magnitude over that predicted by simple thermionic emission calculations [3–8]. Theoretical modelling of tunnelling current depends critically on the calculation of the tunnelling probability of majority carriers through the energy barrier in the semiconductor depletion layer at the metal–semiconductor interface. The transmission coefficient is defined as the ratio of the fluxes due to an incident and a transmitted wave. These wave functions can be found by solving the stationary one-dimensional (1D) Schrödinger equation in the barrier region, which can be achieved using different numerical methods, such as the commonly applied Wentzel–Kramers–Brillouin (WKB) approximation and the transfer matrix method (TMM). The WKB method, however, does not account for wave function reflections; it has limited accuracy for potentials which vary rapidly with the distance. A more general approach is the TMM. The basic principle of this method is the approximation of an arbitrary-shaped energy barrier by a series of barriers with constant or linear potential. However, several authors have noted numerical problems in applying this method for the computation of wave functions [9]. These problems are due to the multiplication of matrices with exponentially growing and decaying states. For thick barriers, this leads to rounding errors which eventually exceed the amplitude of the wave function itself.

An Airy function transfer matrix and WKB tunnelling models have been compared by Vega [10] in the application to Schottky field-effect transistors with and without the incorporation of Schottky barrier lowering (SBL). In this study the author has shown that the WKB model can predict tunnelling current through a Schottky barrier with reasonable accuracy when SBL is excluded. However, the bias voltage used was very low (<3 V) and the Schottky barrier under those conditions is relatively large. Furno [6] in his work have found a main difference between the two approaches WKB and TMM, in particular, at the higher bias.

In this paper, we will focus on a less known, yet powerful, modified Airy function (MAF) method which yields an approximate analytic solution to the 1D time-independent

[3] Author to whom any correspondence should be addressed.

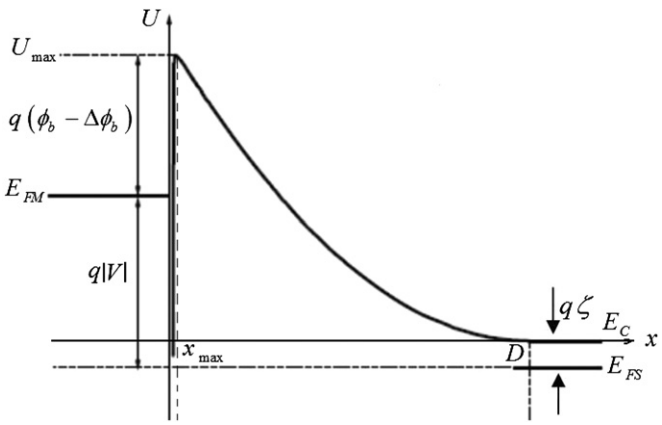

Figure 1. Energy band diagram of the Schottky interface including the image force effects at reverse bias voltage.

Schrödinger equation and a closed form expression for the wave function. The main strength of the Airy function approach is that it provides an exact solution for a linear potential [11–13]. This method was first proposed by Langer in 1931 [14]. Royal [15] revived this method again in 1991. It has been shown to be more accurate than the WKB method in optical waveguide problems, such as the calculation of eigenvalues and eigenfunctions [9]. But its applications, robustness, and advantages have never been properly studied in the tunnelling modelling of Schottky barrier diodes. This is the first use of this technique for the simulation of transmission coefficients in Schottky barrier diodes.

2. Theory and modelling

2.1. Schottky barrier model

The 1D potential barrier profile at the Schottky metal–semiconductor interface is shown in figure 1. The potential energy profile $U(x)$ as a function of the distance from the Schottky interface (located at $x = 0$) can be written as [4, 6]

$$U(x) = \frac{q^2 N_D}{2\varepsilon_s}(D - x)^2 - \frac{q^2}{16\pi\varepsilon_s x}. \tag{1}$$

Where N_D is the semiconductor (n-type) doping concentration, ε_s is the semiconductor permittivity. D is the depletion region width, dependent on the bias voltage V applied to the Schottky contact and on the Schottky barrier height (SBH), ϕ_b according to

$$D = \sqrt{\frac{2\varepsilon_s}{qN_D}(\phi_b - \zeta - V)} \tag{2}$$

where $q\zeta$ is the difference of energy between the conduction band and the equilibrium Fermi level. The first term in equation (1) is the conventional parabolic depletion potential for a Schottky interface, which is referred to the bottom of the conduction band in the neutral semiconductor. The second term is the image force potential term, added to the depletion component as a first-order perturbation. The barrier lowering due to the image charge effect is given by [16]

$$\Delta\phi_B = \left[\frac{q^3 N_D (\phi_b - \zeta - V)}{8\pi^2\varepsilon_s^3}\right]^{1/4}. \tag{3}$$

Location of the potential maxima $x_{\max}$ can be obtained by numerically from the following equation

$$\frac{q^2 N_D}{2\varepsilon_s}(D - x)^2 - \frac{q^2}{16\pi\varepsilon_s x} = 0. \tag{4}$$

The potential energy maximum $U_{\max}$ is given by

$$\begin{aligned} U_{\max}(x_{\max}) &= \frac{q^2 N_D}{2\varepsilon_s}(D - x_{\max})^2 - \frac{q^2}{16\pi\varepsilon_s x_{\max}} \\ &= q\phi_b - q\Delta\phi_b - qV - q\zeta. \end{aligned} \tag{5}$$

2.2. Tunnelling current

The tunnelling carrier transport across the metal–semiconductor interface will be considered in two parts. Carriers can traverse either from the semiconductor to the metal, or vice versa. The corresponding current densities are designated as J_{SM} and J_{MS}, respectively. The observed current density is the algebraic sum of these two components [5, 17]

$$\begin{aligned} J &= J_{SM} - J_{MS} \\ &= \frac{A^* T}{k_B}\int_{E_{\min}}^{U_{\max}} T(E_x)\int_0^{\infty}(f_m(E) - f_s(E))\,\mathrm{d}E_p \end{aligned} \tag{6}$$

where A^* is the effective Richardson constant, T is the temperature, k_B *is* the Boltzmann constant, $f_m(E)$ and $f_s(E)$ are the Fermi–Dirac distribution functions for the metal and the semiconductor, respectively. The total kinetic energy E is decomposed as the sum of E_x, related to the velocity component v_x transversal to the Schottky barrier plane, and E_p, associated to the velocity components parallel to the Schottky interface. In our 1D model, the transmission coefficient (tunnelling probability) $T(E_x)$ is assumed to depend only on the transversal energy component E_x. The WKB tunnelling coefficient is given by

$$T_{WKB} = \theta^2 = \left(\exp\left(-\int_{x_1}^{x_2}\left[\frac{2m^*}{\hbar}(U(x) - E)\right]^{1/2}\mathrm{d}x\right)\right)^2 \tag{7}$$

where, x_1 and x_2 are the two turning points.

An another WKBJ tunnelling coefficient is developed by Ghatak [18] and given by

$$T_{WKBJ} = \frac{1}{\left[\frac{1}{\theta} + \frac{\theta}{4}\right]^2}. \tag{8}$$

The T_{WKBJ} expression is more accurate than the T_{WKB} expression.

The two turning points x_1 and x_2 correspond to the Schottky barrier can be obtained by solving numerically the following equation

$$\frac{q^2 N_D}{2\varepsilon_s}(D - x)^2 - \frac{q^2}{16\pi\varepsilon_s x} = E. \tag{9}$$

2.2.1. Padovani–Straton's formula. Padovani and Stratton [19] analysed tunnelling currents given by equation (6) in Schottky barriers from the standpoint of the field and thermionic-field emission (TFE) using a 1D WKB approximation. However, their analysis ignored image force effects and used a simple parabolic barrier shape.

(a) Field emission (FE). It occurs at low temperatures where most of the electrons originate from the Fermi level of the metal. It was derived by expanding the tunnelling probability in a Taylor series about the Fermi energy of the metal. The current density in the reverse bias applied is expressed by the following equation [19]

$$J_{FE} = \frac{A^*T^2\pi \exp\left[-2q\phi_b^{3/2}/3E_{00}(\phi_b - V)^{1/2}\right]}{k_BT[\phi_b/(\phi_b - V)]^{1/2}\sin\{\pi k_BT[\phi_b/(\phi_b - V)]^{1/2}/E_{00}\}} \tag{10}$$

where E_{00} is a constant related to the WKB expression for the transmission of the barrier and is given as follows

$$E_{00} = \frac{q\hbar}{2}\sqrt{\frac{N_D}{m_e^*\varepsilon_s}}. \tag{11}$$

The maximum temperature for which equation (10) is applicable is given by the condition

$$kT < \left\{E_{00}^{-1}\left[\phi_b/\left(\phi_b - V\right)\right]^{1/2} + (-0.5qE_{00}V)^{1/2}\right\}^{-1}. \tag{12}$$

(b) Thermionic field emission. It occurs at intermediate temperatures where most electrons tunnel at any energy level E_m (above the Fermi level of the metal), constituting the so-called TFE or thermally assisted FE, also utilizing a Taylor expansion about some energy E_m greater than E_{FM}. The current density in the reverse bias applied is expressed by the following equation [19]

$$J_{TFE} = \frac{A^*T}{k_B}\sqrt{\pi E_{00}q\left(-V + \frac{\phi_b}{\cosh^2\left(E_{00}/k_BT\right)}\right)} \times \exp\left(\frac{-q\phi_b}{E_0}\right)\exp\left(-\frac{qV}{\varepsilon'}\right) \tag{13}$$

where

$$\varepsilon' = \frac{E_{00}}{\left(E_{00}/k_BT\right) - \tanh\left(E_{00}/k_BT\right)} \tag{14}$$

$$E_0 = E_{00}\coth\left(\frac{E_{00}}{k_BT}\right). \tag{15}$$

The minimum bias to apply to the diode in order to observe TFE is given by the condition

$$-V > \phi_b + \frac{3E_{00}}{2q}\frac{\cosh^2(E_{00}/k_BT)}{\sinh^3(E_{00}/k_BT)}. \tag{16}$$

The minimum temperature for which equation (13) is applicable is given by the condition

$$k_BT > \left\{E_{00}^{-1}[\phi_b/(\phi_b - V)]^{1/2} + (-0.5qE_{00}V)^{1/2}\right\}^{-1}. \tag{17}$$

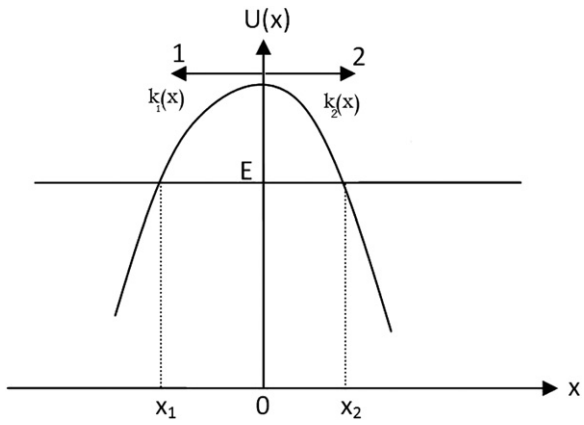

Figure 2. An arbitrary potential function $U(x)$.

2.2.2. Tsu–Esaki's formula. The most prominent and almost exclusively used expression to describe direct tunnelling transitions has been developed by Duke [9] and used by Tsu and Esaki to describe tunnelling through a 1D superlattice [20]. It is commonly known as the Tsu–Esaki expression. The current density of equation (6) reads

$$J_{T\&E} = \frac{A^*T}{k_B}\int_{E_{min}}^{U_{max}} T(E_x)N(E_x)\,dE_x \tag{18}$$

where $N(E_x)$ is the supply function reflecting the difference in the occupation numbers on the two sides of the tunnelling barriers [21] and it evaluates to [3, 4, 20, 22]

$$N(E_x) = \ln\left(\frac{1 + \exp(-q\zeta - E_x)/k_BT}{1 + \exp(-q\zeta - qV - E_x)/k_BT}\right). \tag{19}$$

To calculate the integral in equation (18) we can use the trapeze method given by the expression

$$J_{T\&E} \approx \left(\frac{U_{max} - E_{min}}{N}\right) \times \left((J(E_{min}) + J(E_{max}))/2 + \sum_{i=1}^{N-1} J_i(E_i)\right) \tag{20}$$

where

$$J_i(E_i) = \frac{A^*T}{k_B}T(E_i)N(E_i) \tag{21}$$

And N is the number of intervals.

2.3. Transmission coefficient modelling using MAF method

In this section we are summarized the essential formalism of this method (for more details see [11, 15]). Consider an arbitrary 1D potential of the form as shown in figure 2.

The time-independent Schrödinger equation is

$$\frac{d^2\psi}{dx^2} + k^2(x)\psi = 0 \tag{22}$$

where

$$k(x) = \left[\frac{2m^*}{\hbar}\left(E - U(x)\right)\right]^{1/2}. \tag{23}$$

The MAF solutions of equation (22) are given by

$$\psi(x) = \frac{1}{\sqrt{\xi'(x)}}\left[\text{const}\,Ai(\xi) + \text{const}\,Bi(\xi)\right]. \tag{24}$$

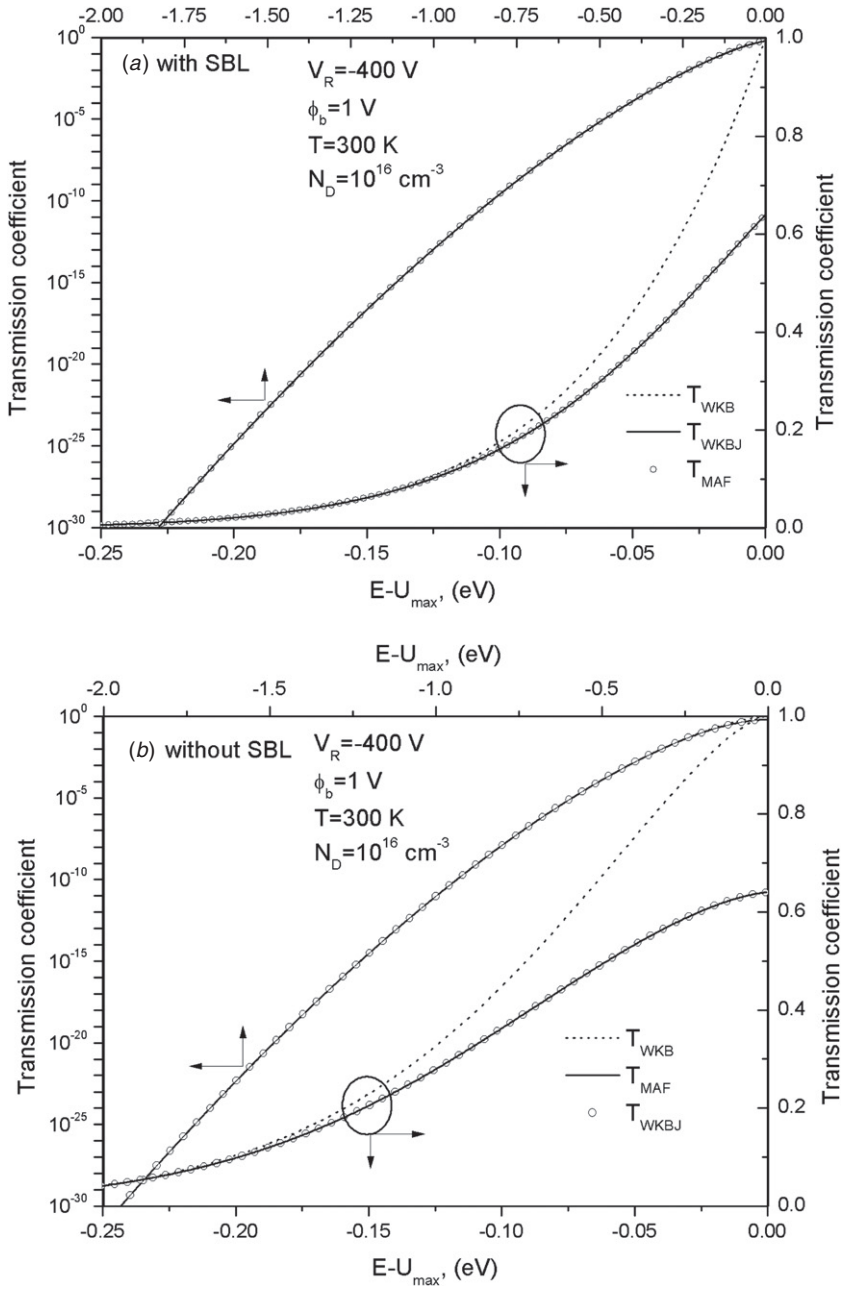

Figure 3. Tunnelling transmission coefficient $T(E)$ as a function of the incident carrier energy relative to the potential energy maximum E–$U_{\max}$. Comparison between the WKB, WKBJ and MAF approaches for an applied reverse bias of −400 V. (Semi-logarithmic scale on the left and linear scale on the right.) (*a*) With SBL, (*b*) without SBL.

The Ai and Bi are the Airy functions given by [23, 24]

$$Ai(x) \cong (4\pi)^{-1/2} x^{-1/4} \exp\left(-\frac{2}{3}x^{3/2}\right) \tag{25}$$

$$Bi(x) \cong \pi^{-1/2} x^{-1/4} \exp\left(\frac{2}{3}x^{3/2}\right). \tag{26}$$

Applying the continuity of $\psi(x)$ and $\psi(x)'$ at $x = 0$ the MAF tunnelling coefficient T_{MAF} is given by

$$T_{\mathrm{MAF}} = \frac{4}{|D_1 + iC_1|^2} \tag{27}$$

where C_1 and D_1 are given by

$$C_1 = \pi K_2[Bi'(\xi_{10}) - K_1 Bi(\xi_{10})] \tag{28}$$

$$D_1 = -\pi K_2[Ai'(\xi_{10}) - K_1 Ai(\xi_{10})] \tag{29}$$

and K_1, K_2 are given by

$$K_1 = \frac{\xi'_{20}}{\xi'_{10}} \frac{-Ai'(\xi_{20}) + iBi'(\xi_{20})}{-Ai(\xi_{20}) + iBi(\xi_{20})} - \frac{\xi''_{20}}{2\xi'_{10}\xi'_{20}} + \frac{\xi''_{10}}{2\xi'^2_{10}} \tag{30}$$

$$K_2 = \sqrt{\frac{\xi'_{10}}{-\xi'_{20}}}[-Ai(\xi_{20}) + iBi(\xi_{20})]. \tag{31}$$

The functions $\xi_1(x)$ in region 1 and $\xi_2(x)$ in region 2 are defined as

$$\xi_1(x) = \left[\frac{3}{2}\int_{x_1}^{x} \sqrt{-k_1^2(x)}\,\mathrm{d}x\right]^{2/3} \quad x_1 \prec x \prec 0 \tag{32}$$

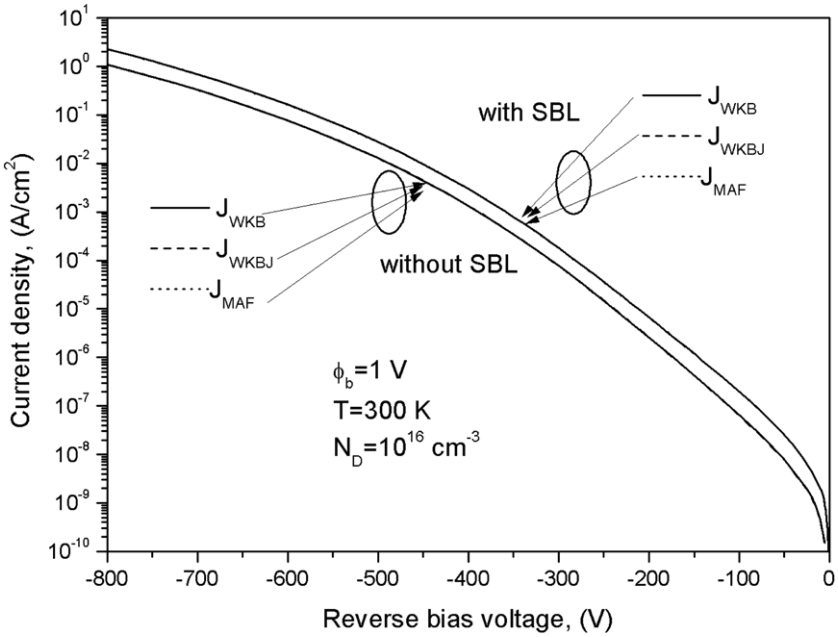

Figure 4. A comparison of the calculated reverse current densities through SBH using Tsu–Esaki's formula with WKB, WKBJ and MAF approaches with and without SBL.

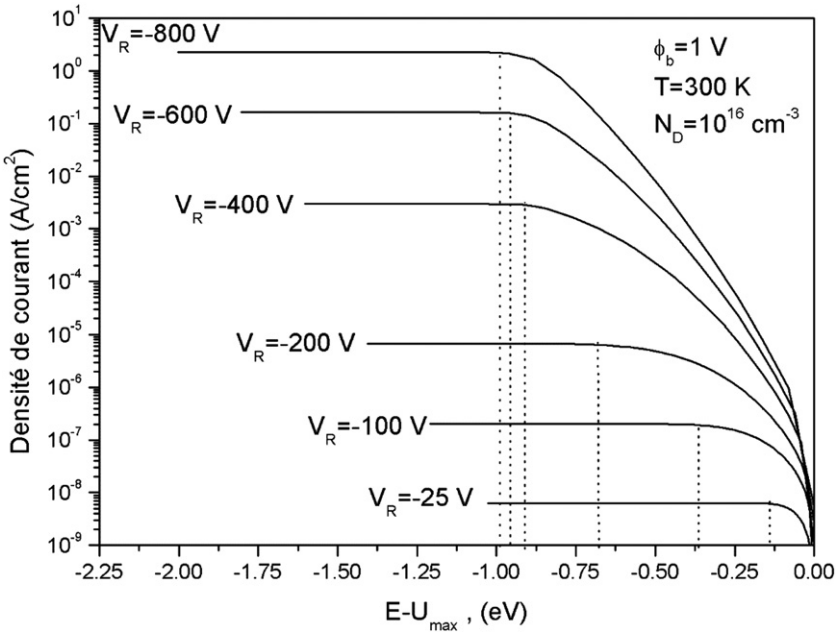

Figure 5. Evolution of the current density as a function of the incident carrier energy relative to the potential energy maximum E–$U_{\max}$ at various reverse bias voltages with SBL.

$$\xi_2(x) = \left[\frac{3}{2}\int_x^{x_2}\sqrt{-k_2^2(x)}\,\mathrm{d}x\right]^{2/3} \quad 0 \prec x \prec x_2. \tag{33}$$

The subscripts '10' and '20' denote the value of the function defined in regions 1 and 2, respectively, at $x = 0$. (In our case at $x = x_{\max.}$) x_1 and x_2 in equation (32) and in equation (33) are the two turning points.

3. Results and discussion

Simulation of reverse characteristics of Schottky diode is performed by effective Richardson constant $A^* = 146$ A cm^{-2} K^{-2}, and the barrier height $\phi_b = 1$ V, these are typical values reported in the literature for experimentally fabricated Schottky diode for Mo/4H-SiC [25, 26], the effective mass $m^* = 0.2$ m [27–29]. The tunnelling transmission probability was calculated according to the WKB, WKBJ approximation and the MAF approach under an applied reverse bias of −400 V with and without the incorporation of SBL as shown in figure 3.

The transmission coefficients calculated by the two methods WKBJ and MAF coincide in a perfect manner on all ranges of energy with and without the incorporation of

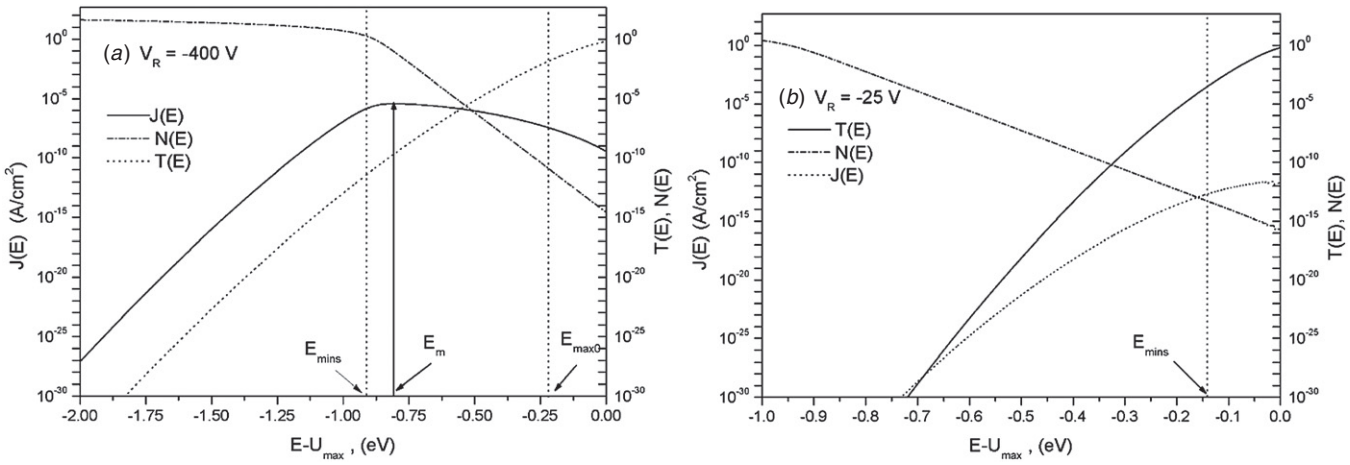

Figure 6. The transmission coefficient, supply function and elementary current density as a function of incident carrier energy relative to the potential energy maximum E–$U_{\max}$ with SBL. (*a*) For $V_R = -400$ V and (*b*) for $V_R = -25$ V with $\phi_b = 1$ V, $N_D = 10^{16}$ cm^{-3}, $T = 300$ K.

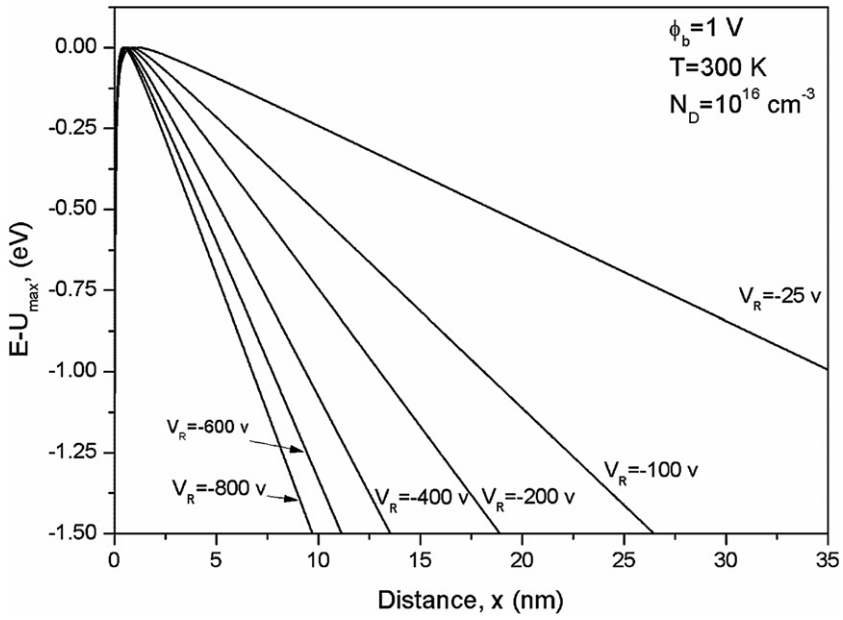

Figure 7. The shape of the energy barrier of Schottky diode at various bias voltages including the effect of the image force lowering, with $\phi_b = 1$ V, $N_D = 10^{16}$ cm^{-3}. The linear coefficient correction equals -0.9999 for all profiles for $x > x_{\max}$).

SBL. For against the transmission coefficient calculated by the WKB method differs slightly in the energy values closer to maximum energy ($U_{\max}$). This range of energy is neglected when we calculate the total current density as we will show below. The reverse current densities calculated accordingly are shown in figure 4. As shown in this figure the current densities calculated by all different methods are identical with each other.

The evolution of the current density as a function of the incident carrier energy relative to the potential energy maximum E–$U_{\max}$ at various bias voltages is shown in figure 5.

The saturation current regime can be obtained by a few eV below the potential energy maximum ($U_{\max}$) for each bias voltage. This means that the energies far from the maximum energy do not contribute in the total current. The potential energy (E_{mins}) that determines the saturation point increases with increasing bias voltage.

Figure 6 shows the variation of the transmission coefficient, the supply function and the elementary current density as a function of energy at $V_R = -400$ V and $V_R = -25$ V.

From these plots we see that the elementary current density increases until reaching a maximum value and decreases approaching the maximum value $U_{\max}$ of the Schottky barrier. The appearance of a maximum of the elementary current density as a function of energy is due to the multiplication of two functions: the first is the coefficient transmission, $T(E)$ which increases and the second function is the supply function, $N(E)$ which decreases as a function of energy. The value E_m which corresponds to the maximum of the elementary current density moves to the $U_{\max}$ when the bias voltage is decreased and it disappears in the lowest bias voltage as shown in figure 6(*b*). It appears in the region $E > U_{\max}$ where the thermionic process is the predominant

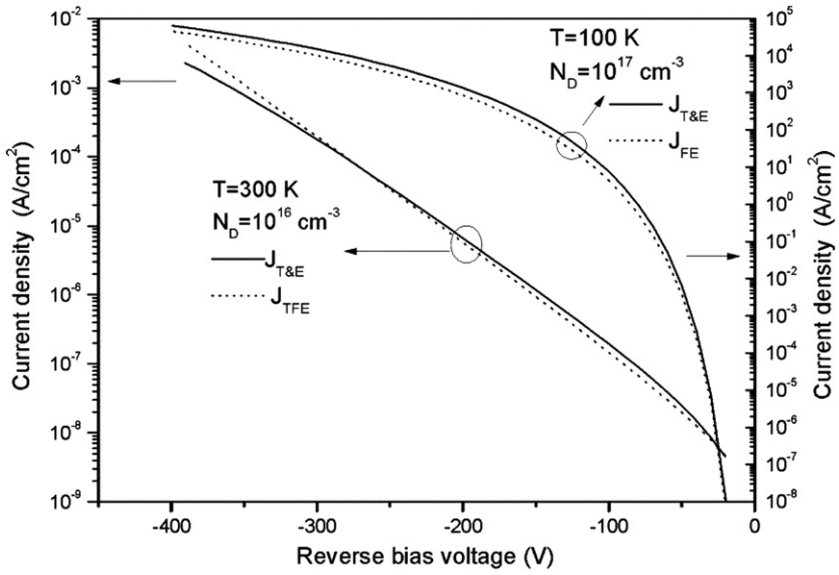

Figure 8. A comparison between the calculated reverse current density using Tsu–Esaki's formula ($J_{T\&E}$) with incorporation of the SBL and reverse current density using Padovani–Straton's formula (field emission—J_{FE}, thermionic field emission—J_{TFE}) for $\phi_b = 1$ V.

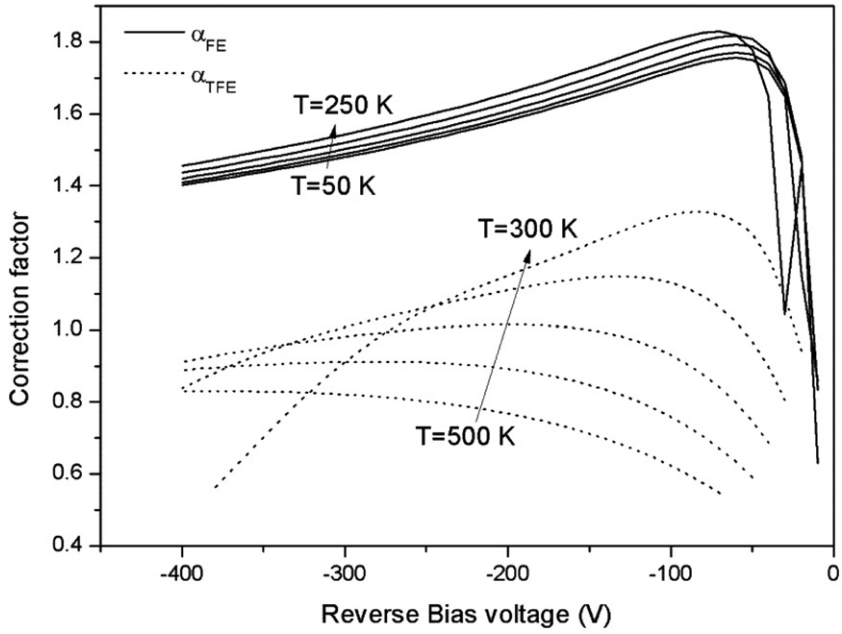

Figure 9. The correction factors (α_{TFE} and α_{FE}) as a function of the reverse bias voltage at various temperatures with $\phi_b = 1$ V, $N_D = 10^{16}$ cm^{-3} for α_{TFE} and $N_D = 10^{17}$ cm^{-3} for α_{FE}.

mechanism. We can note also, that the energy contribution is not symmetrical around E_m. As we mentioned above, the energies below E_{mins} do not contribute in the total current that allow us to neglect also the elementary current densities existing in the other side (in the vicinity of U_{max}; $E > E_{max0}$), which have the same orders of magnitude of the current density below E_{mins}. The shape of the potential barrier in proximity of the Schottky interface is shown in figure 7.

The profile of the potential barrier ($x > x_{max}$) is linear in the region where the tunnelling occurs. In effect, the linear coefficient correction equals -0.9999 for all profiles (-1 for the barriers with no image force effects). This value is much closer to the ideal value -1.

Due to the linear shape of the potential, the accuracy of the MAF method for the linear shape and the total equality for two different methods (WKBJ, MAF) we can conclude that MAF and WKBJ (WKB) approaches are applicable in the case of the Schottky diode barriers.

A comparison between TFE, FE, and this numerical is shown in figure 8. The doping and temperature were chosen so that the FE or TFE occurs only. In the case of TFE, we use $N_D = 10^{16}$ cm^{-3} and $T = 300$ K and for the case of FE we use $N_D = 10^{17}$ cm^{-3} and $T = 100$ K.

It is clear that the numerical approach is close to the Padovan–Straton's formula. The simple difference between them due to the fact that Padovan–Straton's formula does

not include any image force lowering of the barrier and they were derived by considering only the first two terms of the Taylor expansion. We have calculated the correction factor α by dividing the current densities $J_{T\&E}$ by the current densities J_{TFE} (or J_{FE}) and we found that it varies slightly with the doping concentration and temperature. In figure 9 we show the correction factor α_{TFE} and α_{FE} as a function of reverse bias voltage at various temperatures. The correction factor α_{TFE} is much closer to 1 than the factor α_{FE}.

4. Conclusion

The modified Airy function (MAF) method is accurate for the linear-shaped barriers which are the case for the top of the Schottky barrier diode where the tunnelling process occurs. The transmission coefficients calculated by the two methods WKBJ and MAF coincide in a perfect manner on all ranges of energy and bias voltage. This proves well, that the Wentzel–Kramers–Brillouin (WKB) is applicable for the Schottky barrier diode. The WKB method has the advantage over the formalism of Padovani and Stratton in that it is applicable over a wider range of biases and temperature than either the field or thermionic field emission equations for the current density, which must multiply by a correction factor.

References

[1] Mahajan A and Skromme B J 2005 *Solid-State Electron.* **49** 945
[2] Matsunami H 2006 *Microelectron. Eng.* **83** 2
[3] Crofton J and Sriram S 1996 *IEEE Trans. Electron Devices* **43** 2305
[4] Zheng L, Joshi R P and Fazi C 1999 *J. Appl. Phys.* **85** 3701
[5] Blasciuc-Dimitriu C, Horsfall A B, Wright N G, Johnson C M, Vassilevski K V and O'Neill A G 2005 *Semicond. Sci. Technol.* **20** 10
[6] Furno M, Bonani F and Ghione G 2007 *Solid-State Electron.* **51** 466
[7] Oyama S, Hashizume T and Hasegawa H 2002 *Appl. Surf. Sci.* **190** 322
[8] Miller E J, Yu E T, Waltereit P and Speck J S 2004 *Appl. Phys. Lett.* **84** 535
[9] Gehring A and Selberherr S 2004 *IEEE Trans. Device Mater. Reliab.* **4** 306
[10] Vega A R 2006 *IEEE Trans. Electron Devices* **53** 1593
[11] Roy S, Ghatak A K, Goyal I C and Gallawa R L 1993 *IEEE J. Quantum Electron.* **29** 340
[12] Jirauschek C 2009 *IEEE J. Quantum Electron.* **45** 1059
[13] Zhang A, Cao Z, Shen Q, Dou X and Chen Y 2000 *J. Phys. A: Math. Gen.* **33** 5449
[14] Langer R E 1931 *Trans. Am. Math. Soc.* **33** 23
[15] Goyal I C, Gallawa R L and Ghatak A K 1991 *J. Electromagn. Waves Appl.* **5** 623
[16] Rhoderick E H and Williams R H 1988 *Metal–Semiconductor Contact* (Oxford: Oxford University Press) for example
[17] Chang C Y and Sze S M 1970 *Solid-State Electron.* **13** 727
[18] Ghatak A K and Lokanathan S 1984 *Quantum Mechanics: Theory and Applications* 3rd edn (New Delhi: Macmillan India)
[19] Padovani F A and Stratton R 1966 *Solid-State Electron.* **9** 695
[20] Tsu R and Esaki L 1973 *Appl. Phys. Lett.* **22** 562
[21] Gildenblat G 2010 *Compact Modeling: Principles, Techniques and Applications* (Dordrecht: Springer)
[22] Eriksson J, Rorsman N and Zirath H 2003 *IEEE Trans. Microwave Theory Tech.* **51** 796
[23] Vatannia S and Gildenblat G 1996 *IEEE J. Quantum Electron.* **32** 1093
[24] Griffiths D J 1995 *Introduction to Quantum Mechanics* (Upper Saddle River, NJ: Prentice- Hall)
[25] Weiss R, Frey L and Ryssel H 2001 *Appl. Surf. Sci.* **184** 413
[26] Latreche A, Ouennoughi Z, Sellai A, Weiss R and Ryssel H 2011 *Semicond. Sci. Technol.* **26** 085003
[27] Itoh A and Matsunami H 1997 *Phys. Status Solidi a* **162** 389
[28] Roccaforte F 2003 *J. Appl. Phys.* **93** 9137
[29] Götz W, Schöner A, Pensl G, Suttrop W, Choyke W J, Stein R and Leibenzeder S 1993 *J. Appl. Phys.* **73** 3332